

## A novel self-alignment method for high precision silicon diffraction microlens arrays preparation and its integration with infrared focal plane arrays

HOU Zhi-Jin<sup>1\*</sup>, CHEN Yan<sup>1</sup>, WANG Xu-Dong<sup>2</sup>, WANG Jian-Lu<sup>1</sup>, CHU Jun-Hao<sup>1</sup>

- (1. State Key Laboratory of Photovoltaic Science and Technology, Shanghai Frontiers Science Research Base of Intelligent Optoelectronics and Perception, Institute of Optoelectronics, Fudan University, Shanghai 200433, China;  
2. State Key Laboratory of Infrared Physics, Shanghai Institute of Technical Physics, Chinese Academy of Sciences, Shanghai 200083, China)

**Abstract:** Silicon (Si) diffraction microlens arrays are usually used to integrate with infrared focal plane arrays (IRFPAs) to improve their performance. The errors of lithography are unavoidable in the process of the Si diffraction microlens arrays preparation in the conventional engraving method. It has a serious impact on its performance and subsequent applications. In response to the problem of errors of Si diffraction microlens arrays in the conventional method, a novel self-alignment method for high precision Si diffraction microlens arrays preparation is proposed. The accuracy of the Si diffractive microlens arrays preparation is determined by the accuracy of the first lithography mask in the novel self-alignment method. In the subsequent etching, the etched area will be protected by the mask layer and the sacrifice layer or the protective layer. The unprotection area is carved to effectively block the non-etching areas, accurately etch the etching area required, and solve the problem of errors. The high precision Si diffraction microlens arrays are obtained by the novel self-alignment method and the diffraction efficiency could reach 92.6%. After integrating with IRFPAs, the average blackbody responsivity increased by 8.3%, and the average blackbody detectivity increased by 10.3%. It indicates that the Si diffraction microlens arrays can improve the filling factor and reduce the crosstalk of IRFPAs through convergence, thereby improving the performance of IRFPAs. The results are of great reference significance for improving their performance through optimizing the preparation level of micro nano devices.

**Key words:** self-alignment, diffraction microlens arrays, high precision, integration, Si, IRFPAs

## 采用新颖自对准法制备高精度硅衍射微透镜阵列及其与红外焦平面阵列集成

侯治锦<sup>1\*</sup>, 陈艳<sup>1</sup>, 王旭东<sup>2</sup>, 王建禄<sup>1</sup>, 褚君浩<sup>1</sup>

- (1. 复旦大学光电研究院 光伏科学与技术全国重点实验室 上海市智能光电与感知前沿科学研究基地, 上海 200433;  
2. 中国科学院上海技术物理研究所 红外物理全国重点实验室, 上海 200083)

**摘要:** 硅衍射微透镜阵列通常被用来与红外焦平面集成, 从而提高器件性能。在常规光刻法用于制备硅衍射微透镜阵列时, 光刻误差是很难避免的, 这对器件性能及后续应用产生严重的影响。针对此问题, 本文提出一种高精度硅衍射微透镜阵列制备的新颖自对准方法。该方法中硅衍射微透镜阵列的制备精度只由第一次掩膜光刻的精度决定。在后续的刻蚀中, 采用掩膜层和牺牲层或保护层将已刻蚀区域进行保护, 对未保护区域进行刻蚀, 有效地阻挡非刻蚀区域, 精确刻蚀所需刻蚀区域。采用新颖自对准法可以制备出高精度硅衍射微透镜阵列, 其衍射效率可达到 92.6%。与红外焦平面探测器集成后, 平均黑体响应率提高了 8.3%, 平均黑体探测率提高了 10.3%。这表明硅微透镜阵列可以通过会聚作用提高焦平面阵列占空因子, 同时降低串扰, 进而提高焦平面阵列性能。该研究结果对通过优化微纳器件制作水平提升其性能具有重要参考意义。

**关键词:** 自对准; 衍射微透镜阵列; 高精度; 集成; 硅; 红外焦平面阵列

Received date: 2023-10-19, revised date: 2023-12-20

收稿日期: 2023-10-19, 修回日期: 2023-12-20

**Foundation items:** Supported by the National Natural Science Foundation of China (62105100), the National Key research and development program in the 14th five year plan (2021YFA1200700)

**Biography:** Hou Zhi-Jin (1982-), male, Xiaoyi, Shanxi, China, senior Engineer, PhD. He is mainly engaged in the application research of infrared detectors and new optoelectronic devices. Email: zhijinhou@fudan.edu.cn

\*Corresponding author: E-mail: zhijinhou@fudan.edu.cn

中图分类号: TN215 文献标识码: A

## Introduction

Infrared focal plane arrays (IRFPAs) have the advantages of high sensitivity, good environmental adaptability, and strong anti-interference. They are widely used in military and civilians such as defense weapons, infrared remote sensing and meteorological environment<sup>[1-6]</sup>. As the scale of IRFPAs is getting larger and larger and the size of the elements are getting smaller and smaller, the filling factor of the IRFPAs is getting smaller and smaller. For example, the size of the elements of the IRFPAs is  $25\ \mu\text{m} \times 25\ \mu\text{m}$ , the size of mesa of the IRFPAs is  $20\ \mu\text{m} \times 20\ \mu\text{m}$ , so the filling factor of the IRFPAs is  $(20\ \mu\text{m} \times 20\ \mu\text{m}) / (25\ \mu\text{m} \times 25\ \mu\text{m})$ , and the calculation which can be seen is only 64%. Low-filled factor not only affects the performance of the IRFPAs, but also restrict its systematic application.

The diffraction microlens arrays can be used to improve the filling factor of the IRFPAs<sup>[7-10]</sup>. The diffraction microlens arrays is a kind of relief-type pure phase diffraction optical elements with small advantages such as small volume, high integration, high diffraction efficiency, and large filling factor. The methods of the diffraction microlens arrays preparation are mainly binary optical technology, laser direct writing technology, and grayscale mask technology<sup>[11-17]</sup>. Most of the diffraction microlens arrays preparation adopt binary optical technology containing photoresists and etching technology. The diffraction microlens arrays using the binary optical technology is easy to be neat and sharp. The filling factor of the diffraction microlens arrays can reach 100%. The diffraction microlens arrays have many other advantages, such as, light weight, low cost, easy to miniature and array.

The diffraction microlens arrays based on Si materials are usually used to integrate with IRFPAs to improve their performance. On one hand, it can optimize the stress of IRFPAs by using the Si (microlens arrays) - semiconductor -Si (readout circuit) structure to solve the chip cracking problem. On the other hand, the light can be collected to the elements of IRFPAs by the convergence of the microlens arrays to improve the performance of the IRFPAs.

The diffraction microlens array for the IRFPAs is usually prepared by the conventional engraving method of the binary optical technology. As the size of element of the IRFPAs is getting smaller and smaller, the corresponding radius of each zone of the Si diffraction microlens arrays is also smaller and smaller. At the same time, the size of the lithographic and etching areas is getting smaller and smaller. It brings many errors happening of the Si diffraction microlens arrays preparation. It has a serious impact on the performance of the Si diffraction microlens arrays and the subsequent application. In this paper, the errors of Si diffraction microlens array preparation in the conventional method are analyzed.

The high precision Si diffraction microlens array is fabricated by the proposed novel self-alignment method. The IRFPA integrated with the Si diffraction microlens array is studied. The results are of great reference significance for improving the performance of micro nano devices by optimizing the production level to meet the system application requirements.

## 1 Analysis of the errors of Si diffraction microlens arrays preparation in the conventional method

The conventional method of diffraction microlens arrays preparation includes three sets of engravings and three etching. The main contents of each etching include rotating the photoresist on the surface of the clean silicon base, using a lithographic mask for lithographic, and exposing the erosion area for etching.

In the process of diffraction microlens arrays preparation by the conventional method, it has a problem of alignment deviation of photocalation, as shown in Figure 1. Figure 1 shows that the graphic of chip after the second etching in the conventional method observed by a microscope. After many experiments, it is found that the phenomenon is more common in the engraving, especially it is more significant in the third etching. Therefore, the errors generated by the conventional method is analyzed, as shown in Figure 2.

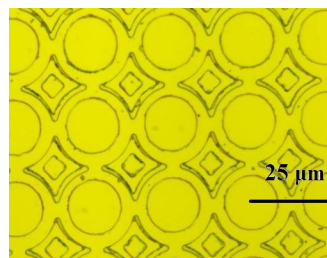


Fig. 1 The microscope graphic of chip after the second etching in the conventional method

图1 常规法二次刻蚀后的芯片图

Figure 2 shows that the analysis of the errors of Si diffraction microlens arrays preparation in the conventional method. It is difficult to engrave when the conventional method is applied to diffraction microlens arrays with the size of element  $25\ \mu\text{m} \times 25\ \mu\text{m}$ . On the one hand, there is a problem with excessive development or lack of appearance during the lithography process. It brings that the radius of zones of diffraction microlens arrays between the actual graphic and the original design will be different, resulting in excess zones on the edge. The preparation accuracy will affect the performance of Si diffraction microlens arrays. On the other hand, it is very difficult by using this method for the lithography alignment of small elements. If the error of zones occurs, it will make lithography alignment more difficult, result-

ing in protrusions or depression on the edge, which will affect the performance of the diffraction microlens arrays.

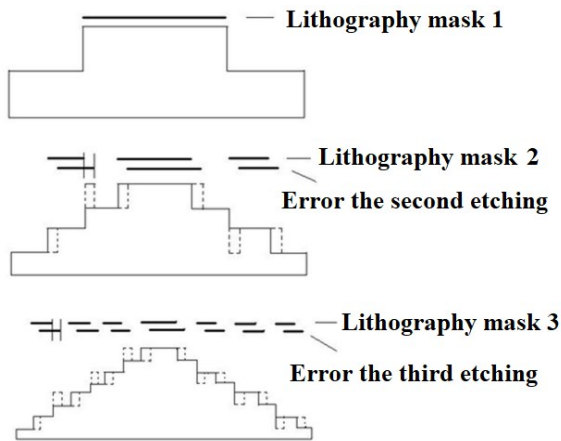


Fig. 2 The analysis diagram of the errors of Si diffraction microlens arrays preparation in the conventional method  
图2 硅微透镜常规法制作误差分析图

## 2 A novel self-alignment method for high precision Si diffraction microlens arrays preparation

The errors are unavoidable in the process of the Si diffraction microlens arrays preparation in the conventional method. The double-sided exposure method<sup>[18]</sup> has been reported to avoid errors, but it only applies to the quartz glass and other materials that transparent ultraviolet light, and it is not suitable for Si and other materials that are not penetrated. Therefore, how to prepare high-precision diffraction microlens arrays based on materials that are opaque to ultraviolet light such as Si has become a difficult research point.

In response to this problem, a novel self-alignment method is proposed to achieve high precision Si diffraction microlens arrays preparation in this article. The process in the novel self-alignment method is introduced and the Si diffraction microlens array is prepared. The appearance of the zones of the Si diffraction microlens array is studied by high power microscope and tested by the optical testing system.

### 2.1 The novel self-alignment method and parameter design

The etched area is protected and the non-protected area is etched in the novel self-alignment method, as shown in Figure 3.

The experimental steps are as follows:

① Sacrifice layer and chromium are made. Negative lithography is used as a sacrifice layer. The chromium window is made by engraving and wet eroding. Then the sacrifice layer window and the second, fourth, and sixth zones are generated by the reactive ion etching in turn. In this step, the edge of each zone of the diffraction microlens arrays is determined by the edge of wetting etching of the chromium, as shown in Figure 3 (a).

② The fourth and eighth zones are generated by the

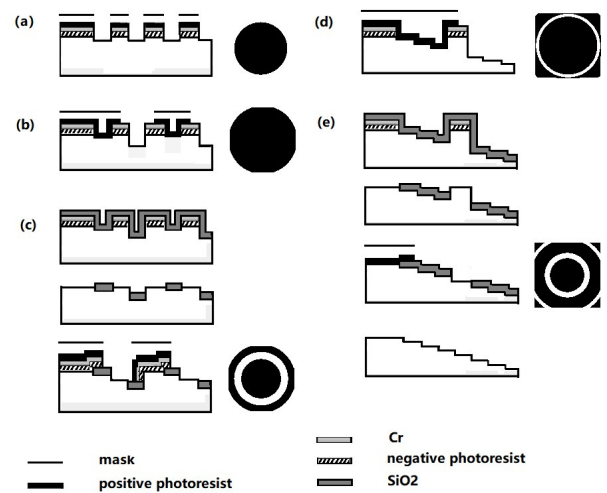


Fig. 3 The schematic diagrams of a novel self-alignment method; (a) the first etching; (b) the second etching; (c) the third etching; (d) the fourth etching; (e) the fifth etching  
图3 新颖自对准法示意图: (a)一次刻蚀; (b)二次刻蚀; (c)三次刻蚀; (d)四次刻蚀; (e)五次刻蚀

reactive ion etching. The edge of the zones is determined by the edge of the mask layer and the wetting etching of the chromium in past step, as shown in Figure 3 (b).

③ The protective layer is made. After the sacrifice layer is stripped off, the protective layer is left. Then the sacrifice layer and chromium are made again. The third and seventh zones are generated by the reactive ion etching. The edge of the zones is determined by the edge of the mask layer and protective layer. In this step, silicon dioxide is used as a protective layer, as shown in Figure 3 (c).

④ The protective layer is corroded. The protective layer silicon can be removed by corrosion, and the surface coverage can be removed together. The sixth, seventh, and eighth zones are generated by the reactive ion etching. The edge of the zone is determined by the edge of the mask layer and the wetting etching of the chromium in past step, as shown in Figure 3 (d).

⑤ The protective layer is made again. After the sacrifice layer is stripped off, the protective layer is left. The fifth zone is generated by the reactive ion etching. The edge of the zone is determined by the edge of the mask layer and protective layer, as shown in Figure 3 (e).

According to the above method, the Si diffraction microlens arrays are obtained. There are no errors in the novel self-alignment method. But it needs to use more lithographic masks than before.

It can be seen in Figure 3 that in order to obtain the high-precision Si diffraction microlens arrays, compared with the conventional method, the novel self-alignment method needs to be eroded several times. Referring to the double-sided exposure method, five lithographic masks are required. Each etch depth is different. The comparison of parameter design value is shown in Table 1. In Table 1, the etching depths of the conventional method are 0.868  $\mu\text{m}$ , 0.434  $\mu\text{m}$ , 0.217  $\mu\text{m}$ , and the

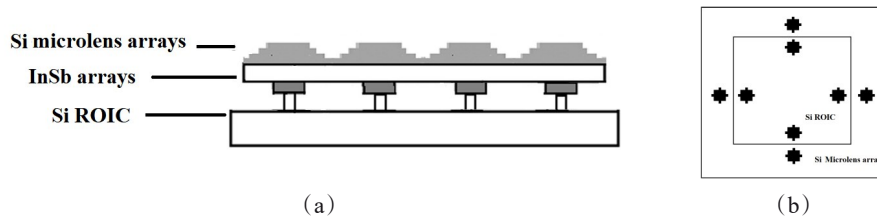


Fig. 4 (a) Elements alignment configuration; (b) alignment marking for Si diffractive microlens arrays and IRFPAs  
图4 硅衍射微透镜阵列与焦平面探测器 (a) 单元对准结构示意图; (b) 对准标记

etching depths of the novel self-alignment method are  $0.217\ \mu\text{m}$ ,  $0.434\ \mu\text{m}$ ,  $0.434\ \mu\text{m}$ ,  $0.868\ \mu\text{m}$ , and  $0.868\ \mu\text{m}$ . The radius of each zone is same, with  $6.2\ \mu\text{m}$ ,  $8.8\ \mu\text{m}$ ,  $10.8\ \mu\text{m}$ ,  $12.45\ \mu\text{m}$ ,  $13.95\ \mu\text{m}$ ,  $15.3\ \mu\text{m}$ ,  $16.5\ \mu\text{m}$ ,  $17.7\ \mu\text{m}$ . The minimum zone width is  $1.2\ \mu\text{m}$ .

**Table 1 Comparison of parameter design value of Si diffraction microlens arrays preparation by the conventional method and the novel self-alignment method**

表1 常规法与新颖自对准法制备硅微透镜阵列的参数设计值对比

	Conventional method	Novel self-alignment method
Size of element	$25\ \mu\text{m} \times 25\ \mu\text{m}$	$25\ \mu\text{m} \times 25\ \mu\text{m}$
Pitch of two neighbor elements	$25\ \mu\text{m}$	$25\ \mu\text{m}$
Middle wave band (Center wavelength)	$3\text{--}5\ \mu\text{m}$ ( $4.2\ \mu\text{m}$ )	$3\text{--}5\ \mu\text{m}$ ( $4.2\ \mu\text{m}$ )
The refractive index of Si	3.42	3.42
The radius of each zone	$6.2\ \mu\text{m}$ , $8.8\ \mu\text{m}$ , $10.8\ \mu\text{m}$ , $12.45\ \mu\text{m}$ , $13.95\ \mu\text{m}$ , $15.3\ \mu\text{m}$ , $16.5\ \mu\text{m}$ , $17.7\ \mu\text{m}$ .	$6.2\ \mu\text{m}$ , $8.8\ \mu\text{m}$ , $10.8\ \mu\text{m}$ , $12.45\ \mu\text{m}$ , $13.95\ \mu\text{m}$ , $15.3\ \mu\text{m}$ , $16.5\ \mu\text{m}$ , $17.7\ \mu\text{m}$ .
The depth of each etching step	$0.868\ \mu\text{m}$ , $0.434\ \mu\text{m}$ , $0.217\ \mu\text{m}$ (Three etching)	$0.434\ \mu\text{m}$ , $0.868\ \mu\text{m}$ , $0.868\ \mu\text{m}$ (Five etching)
The minimum zone width	$1.2\ \mu\text{m}$	$1.2\ \mu\text{m}$

## 2.2 Preparation, test and integration

AZ1500 is used as photoresist. SI500E type equipment is used as reactive ion etching. The etching conditions are as follows: the gas flow of  $\text{CHF}_3$ :  $\text{O}_2$  is 24 ml:6 ml, the ICP source power is 400 W, the RF source power is 150 W, and the pressure of reaction room is 0.5 Pa. The Si diffraction microlens array is prepared by the novel self-alignment method. In order to increase the transmission of the Si diffraction microlens array, the double-sided transplanted film is coated. The zones of the Si dif-

fraction microlens array are tested with the help of Alpha Step 500 steps and Eeco's Wyko HD300 contours. The surface morphology is tested with a stereomicroscope. The focal point and optical energy distribution are tested by the optical testing system.

The Si diffractive microlens array is thinned and polished to focus on a point. The alignments are designed and prepared on the surface of the readout circuit of IRFPAs and Si diffraction microlens arrays. The glue without bubbles is used to couple the Si diffractive microlens array and the IRFPAs. Each element of Si diffraction microlens array and each element of the IRFPAs will be aligned according to the alignment marking, as shown in Figure 4. The integration IRFPAs detector is encapsulated in metal shell and characterized by IRFPAs test-bench.

## 3 Result and discussion

The microscope graphics and unit surface profile of Si diffractive microlens arrays are shown in Figure 5 and Figure 6, respectively.

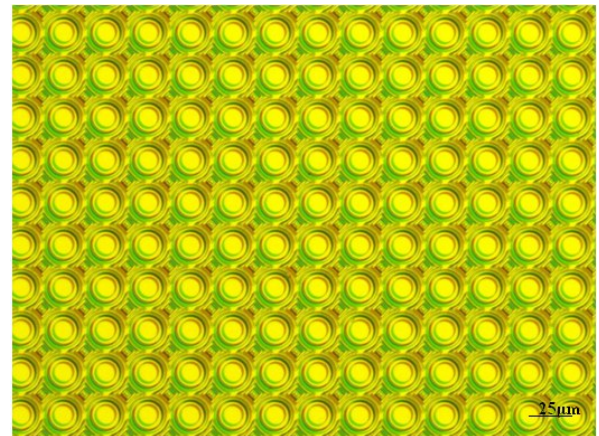


Fig. 5 The microscope graphics of Si diffractive microlens arrays  
图5 硅衍射微透镜阵列表面形貌

From Figure 5 and Figure 6, it can be seen that the novel self-alignment method has highly accurate. It is because the accuracy of the Si diffractive microlens arrays is determined by the accuracy of the first lithography mask. In the subsequent etching, the etched area will be protected by the mask layer and the sacrifice layer or the protective layer. The unprotection area is carved to effec-

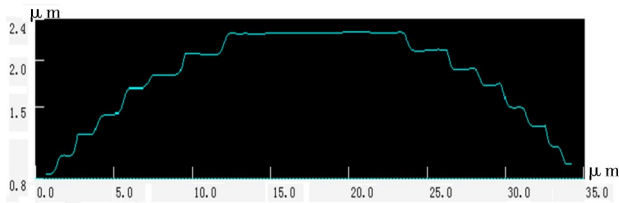


Fig. 6 The unit surface profile of Si diffractive microlens arrays  
图6 硅衍射微透镜阵列单元表面轮廓

tively block the non-etching areas, accurately etch the etching area required, and solve the problem of errors that are easily prone to Si diffractive microlens array preparation in the process of mask alignment, lithography, and etching. It meets the high precision requirements in the process of making Si diffractive microlens arrays preparation, and effectively guarantees and improves the optical properties such as the diffraction efficiency of the Si diffractive microlens arrays.

Figure 7 shows the schematic diagram of optical testing system. The prepared Si diffractive microlens array is tested by the optical testing system. Local focal spots and randomly selected a focal point intensity distribution of Si diffractive microlens arrays are shown in Figure 8. The diffraction efficiency of the Si diffractive microlens arrays is calculated by the following formula:

$$\eta = E_d / E_p = (E_p - E_b) / E_p \quad (1)$$

The diffraction efficiency  $\eta$  is the ratio of  $E_d$  which is the light energy in the main diffraction order range to  $E_p$  which is the total light energy of the exit surface after deducting the reflection and absorption of the flat substrate. Here, a background deduction method is used for the diffraction efficiency calculation, where  $E_d$  which is the light energy in the main diffraction order range is the difference between  $E_p$  which is the total light energy of the exit surface after deducting the reflection and absorption of the flat substrate and  $E_b$  which is the light energy of background noise.

According to formula (1), the diffraction efficiency of the Si diffractive microlens arrays is 92.6%. Compared with the theoretical eight-level diffraction efficiency, it is only 2.4% lower.

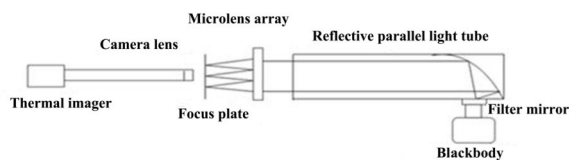
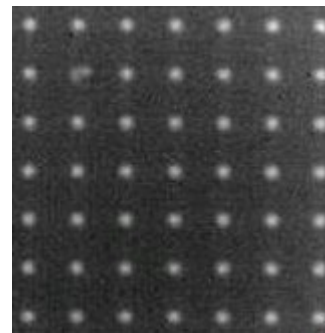
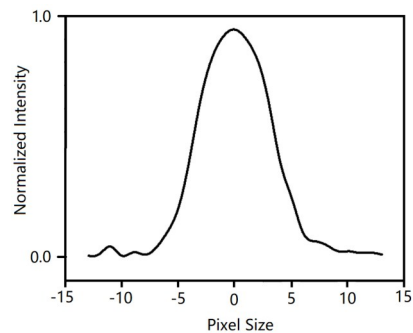


Fig. 7 Schematic diagram of optical testing system  
图7 光学测试系统

The prepared Si diffractive microlens array is integrated with InSb IRFPAs with the size of element  $25 \mu\text{m} \times 25 \mu\text{m}$ . It is encapsulated in metal shell and characterized by IRFPAs test-bench. Table 2 is comparison of the performance of the IRFPAs before and after integrating Si diffraction microlens arrays. According to the calculated results of the Table 2, the average blackbody responsivity



(a)



(b)

Fig. 8 (a) Local focal spots; (b) randomly selected a focal point intensity distribution of Si diffractive microlens arrays  
图8 硅衍射微透镜阵列: (a)局部焦点; (b)随机选定某焦点光能分布

increased by 8.3%, and the average blackbody detectivity increased by 10.3%. The increase in the average blackbody detectivity is greater than the increase in the average blackbody responsivity. It indicates that the Si diffraction microlens arrays can improve the filling factor and reduce crosstalk of IRFPAs through convergence, thereby improving the performance of the IRFPAs.

Table 2 Comparison of the main performance of the InSb IRFPAs before and after integrating with Si diffraction microlens array

表2 集成硅衍射微透镜阵列前后InSb红外焦平面主要性能对比

Indicator	Before integrating with Si diffraction microlens arrays	After integrating with Si diffraction microlens arrays
Average blackbody responsivity	$7 \times 10^7 \text{ cm} \cdot \text{Hz}^{1/2} \cdot \text{W}^{-1}$	$7.58 \times 10^7 \text{ cm} \cdot \text{Hz}^{1/2} \cdot \text{W}^{-1}$
Average blackbody detectivity	$1.16 \times 10^{10} \text{ cm} \cdot \text{Hz}^{1/2} \cdot \text{W}^{-1}$	$1.28 \times 10^{10} \text{ cm} \cdot \text{Hz}^{1/2} \cdot \text{W}^{-1}$

## 4 Conclusion

In response to the problem of errors of Si diffraction microlens arrays in the conventional engraving method, the novel self-alignment method to realize the of high pre-

cision Si diffraction microlens arrays preparation is proposed. The experimental results show that the Si diffraction microlens arrays using the novel self-alignment method has high accuracy, and its diffraction efficiency can reach 92.6%. After integrating with IRFPAs, the average blackbody responsivity increased by 8.3%, and the average blackbody detectivity increased by 10.3%. The integration optimization between the Si diffraction microlens arrays and the IRFPAs will be the key to application and the focus of next research. The results have important reference significance for improving their performance through optimizing the preparation level of micro nano devices.

## References

- [1] Lei W, Antoszewski J, and Faraone L. Progress, challenges, and opportunities for HgCdTe infrared materials and detectors [J]. *Appl. Phys. Rev.*, 2015, **2**: 041303.
- [2] Hu Wei-Da, Liang Jian, Yue Fang-Yu, et al. Recent progress of subwavelength photo trapping HgCdTe infrared detector [J]. *J. Infrared Millim. Waves* (胡伟达, 梁健, 越方禹等. 新型亚波长陷光结构 HgCdTe 红外探测器研究进展. *红外与毫米波学报*), 2016, **35** (1): 25-36.
- [3] Rogalski A, Antoszewski J, and Faraone L. Third-generation infrared photodetector arrays [J]. *J. Appl. Phys.* 2009, **105**: 091101.
- [4] Rogalski A. *Infrared Detectors* [M]. New York, CRC Press, 2011.
- [5] HOU Zhi-Jin, FU Li, LU Zheng-Xiong, et al. Causes and characteristics of indium bump defects in InSb focal plane array [J]. *J. Infrared Millim. Waves* (侯治锦, 傅莉, 鲁正雄等. InSb 面阵探测器铜柱缺陷成因与特征研究. *红外与毫米波学报*), 2018, **37**(3): 227-233.
- [6] HOU Zhi-Jin, FU Li, SI Jun-Jie, et al. Identification and Orientation of Connected Defective Elements in FPA [J]. *J. Infrared Millim. Waves* (侯治锦, 傅莉, 司俊杰等. 面阵探测器相连缺陷元识别定位. *红外与毫米波学报*), 2017, **36**(2): 208-213.
- [7] Guo N, Hu W D, Chen X S, et al. Optimization for mid-wavelength InSb infrared focal plane arrays under front-side illumination [J]. *Opt. Quant. Electron.* 2013, **45** (7): 673-679.
- [8] Guo N, Hu W D, Chen X S, et al. Optimization of microlenses for InSb infrared focal-plane arrays [J]. *J. Electron. Mater.* 2011, **40**: 1647-1650.
- [9] ZUO Hai-Jie, YANG Wen, ZHANG Jiang-Yong, et al. Focal shift of silicon microlens array in mid-infrared regime [J]. *J. Infrared Millim. Waves* (左海杰, 杨文, 张江勇等. 中红外硅微透镜阵列的离焦效应. *红外与毫米波学报*), 2017, **36**(2): 149-153.
- [10] BAI J, HU W D, GUO N, et al. Performance optimization of InSb infrared focal plane arrays with diffractive microlenses [J]. *Journal of ELECTRONIC MATERIALS*, 2014, **43**(8): 2795-2801.
- [11] Li M J, Yang Q, Bian H, et al. Microlens arrays enable variable-focus imaging [J]. *Optics & Laser Technology*. 2022, **153**: 108260.
- [12] Chen P C, Yeh C S, Hsieh C. Defocus digital light processing stereolithography for rapid manufacture of microlens arrays [J]. *Sensors & Actuators: A. Physical*. 2022, **345**: 113819.
- [13] Zhong Y, Yu H B, Wen Y D, et al. Novel Optofluidic Imaging System Integrated with Tunable Microlens Arrays [J]. *ACS Applied Materials & Interfaces*. 2023, **15** (9): 11994-12004.
- [14] Zhang J G, Ma S Y, Tan W, et al. Random spherical microlens array fabricated by elliptical vibration diamond cutting and molding [J]. *Applied Optics*. 2023, **13** (62): 3445-3453.
- [15] Banerji S, Meem M, Majumder A. Super-resolution imaging with an achromatic multi-level diffractive microlens array [J]. *Optics letters*, 2020, **45**(22): 6158-6161.
- [16] LI H, LI T, CHEN S, et al. Photoelectric hybrid neural network based on ZnO nematic liquid crystal microlens array for hyperspectral imaging [J]. *Optics Express*, 2023, **5**(31): 7643-7658.
- [17] Wu M H, Paul K E, Yang J, et al. Fabrication of frequency selective surfaces using microlens projection photolithography [J]. *Applied Physics Letters*, 2002, **80**(19): 3500-3502.
- [18] Chen S H, Yi X J, Ma H. A novel method of fabrication of microlens arrays [J]. *Infrared Physics & Technology*, 2003, **44**: 133-135.